Joint 48th IEEE Conference on Decision and Control and
28th Chinese Control Conference
Shanghai, P.R. China, December 16-18, 2009

Stability Analysis of Grasped Object by Soft-Fingers with 3-Dimensional Deformation based on Moment Stability

Akira Nakashima and Yoshikazu Hayakawa

Abstract— **This paper analyze stability of an object grasped by soft-fingers in 3-dimensional space based on moment stability. We firstly define the moment stability as a criterion for stability of a grasped object when the object is perturbed for the orientation. In detail, the moment stability means that the grasping force can be the restoring force when the object is perturbed. Based on the moment stability, the stability condition of an object grasped by hard-fingers is derived. We indicate that contact points to satisfy the condition are restricted to upper locations of the center of mass and the class of the object shape is only a kind of hollow objects. Next, the condition of an object grasped by semispherical soft-fingers thirdly is considered. Two-fingered grasp by soft-fingers can satisfy the force-closure which is traditional major criterion for static grasp. The consideration shows a novel result that two-fingered grasp can satisfy the moment stability with only two fingers while the hard-fingers need at least three numbers for the force-closure and can not satisfy the moment stability. On the other hand, it is indicated that the torsion moments do not effect on the moment stability well and it is necessary to add the third finger in a condition of the contact points. Numerical examples finally are shown.**

I. Introduction

Many researchers have tried to introduce robots into human's daily environments. Since the robots are aimed to do various tasks instead of human, multi-fingered robot hands are effective as end-effectors. Multi-fingered robot hands have capability to grasp variously-shaped objects because the hands can grasp with multi contacts and can control grasping force via multi joint inputs.

There are many research for grasp stability of an object grasped by balanced contact forces when the object is perturbed from its equilibrium point. When the object is displaced and the balanced forces are invariant, the forces generate the resultant force and moment to the object. This is referred to as the *stiffness effect* and is a direct measure of quasi-static grasp stability [1]. Cutkosky and Kao [2] derived the stiffness matrix between resultant force/moment and small displacement of a grasped object as a function of geometry of the grasped object and contact condition. Montana [3] analyzed the stiffness effect of an grasped object with rolling contact in 2D space concerned with the curvature of the object. Maekawa et al. [4] analyzed the stiffness effect with rolling contact in 3D space and derived the stiffness matrix to evaluate the stiffness effect of the translation/rotation of the object and the contact movement due to the rolling contact. Since it is assumed that finger-tips are rigid bodies in the all studies, the stiffness effect destabilize the grasped object except for the stiffness effect due to rolling contact [4]. While these studies do not control contact forces, there are studies where the stiffness effect is controlled by contact forces to stabilize a grasped object around its equilibrium [5], [6], [7]. In this paper, we concentrate on the stiffness effect without controlling contact forces.

Recently, soft-fingers made from soft materials have been studied. Compared with hard-fingers made from hard materials, the soft-fingers have a lot of advantages [8]: the contact friction is larger than that of the hard-finger since the contact is surface; the soft-finger can reduce the impact force in contact establishment; it can fit on various shapes of the object; there exists moment friction about the contact normal. Inoue et al. [9], [10], [11], [12] proposed a parallel distributed deformation model of a semispherical soft fingertip and considered stability of two-fingered grasp based on the local minimum elastic energy with the rolling contact in two-dimensional space. On the other hand, Nakashima et al. [13] proposed a radial distributed deformation model of a semispherical soft fingertip and showed a stability condition of two-fingered grasp to satisfy the *moment stability* based on the stiffness effect. These studies are restricted in 2-dimensional space and can not consider the moment friction about the contact normal because of 2-dimensional deformation model. This moment is new feature in 3-dimensional deformation of a soft-finger and one of the advantages of a soft-finger as mentioned previously. Two-fingered grasp by soft-fingers can satisfy the *force-closure* [14], which is a traditional major criterion for static grasp. However, it is not evident how the moment effects on restoring force when a grasped object is perturbed.

In this paper, we study stability of an object grasped by soft-fingers in 3-dimensional space based on the stiffness effect. The study [4] showed that the stiffness effect due to the object rotation is much larger than the one due to the object translation and the stiffness effect due to the rolling contact stabilize the object. Therefore, we consider the object rotation and the rolling contact. We firstly define the moment stability as a criterion for stability of a grasped object when the object is perturbed for the orientation. Based on the moment stability, the stability condition of an object grasped by hard-fingers is derived. The problem setting are a specified case of the analysis in Ref. [4]. We indicate that contact points to satisfy the condition are restricted to upper locations from the center of mass and the class of the object shape is only a kind of hollow objects. Next, the condition of an object grasped by semispherical soft-fingers

Authors are with Mechanical Science and Engineering, Graduate School of Engineering, Nagoya University, Furo-cho, Chikusa-ku, Nagoya, Japan akira@haya.nuem.nagoya-u.ac.jp, and Y. Hayakawa is also with RIKEN-TRI Collaboration Center, RIKEN, 2271-103, Anagahora, Shimoshidami, Moriyama-ku, Nagoya, Japan.

978-1-4244-3872-3/09/$25.00 ©2009 IEEE

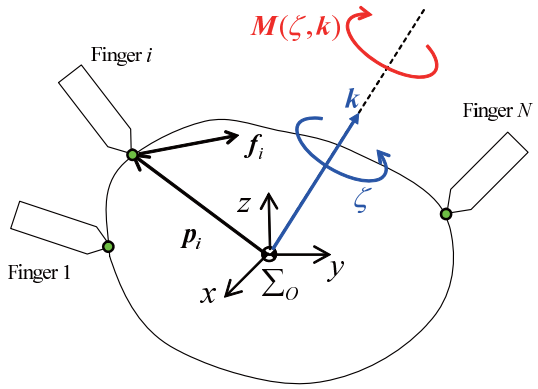

Fig. 1. An object grasped by hard-fingers.

thirdly is considered. A 3-dimensional deformation model of a soft-finger and the contact kinematics with the deformation are utilized which has been proposed in [15]. Two-fingered grasp by soft-fingers can satisfy the force-closure which is traditional major criterion for static grasp. The consideration shows a novel result that two-fingered grasp can satisfy the moment stability with only two fingers while the hard-fingers need at least three numbers for the force-closure and can not satisfy the moment stability. On the other hand, it is indicated that the torsion moments do not effect on the moment stability very well and it is necessary to add the third finger in a condition of the contact points. Numerical examples finally are shown for the consideration.

II. Stability Analysis of Hard-Finger Grasp

We firstly analyze stability of an object grasped by a pair of hard-fingers in 2D space as shown in Fig. 1. The fingers and object are rigid bodies and the fingers are pointy. Σ_O is the reference frame attached at the center of mass of the object. Note that vectors without left superscripts are expressed in Σ_O. $\boldsymbol{f}_i,\ \boldsymbol{p}_i \in \mathbb{R}^3\ (i = 1, \cdots, N)$ are the contact force and the position vector at the ith contact point respectively. The grasp of the object is defined as the following equilibrium equations of force and moment:

$$\sum_{i=1}^{N} \boldsymbol{f}_i + m\boldsymbol{g} = \boldsymbol{0}, \tag{1}$$

$$\sum_{i=1}^{N} \boldsymbol{S}(\boldsymbol{p}_i)\boldsymbol{f}_i = \boldsymbol{0}, \tag{2}$$

where m is the mass of the object, $\boldsymbol{g} := [0\ 0\ g]^{\mathrm{T}}$, $g = -9.8$ [m/s^2] is the gravitational vector and $\boldsymbol{S}(\boldsymbol{p}_i) \in \mathbb{R}^{3\times3}$ is the skew-symmetric matrix defined as

$$\boldsymbol{S}(\boldsymbol{p}_i) := \begin{bmatrix} 0 & -p_{z_i} & p_{y_i} \\ p_{z_i} & 0 & -p_{x_i} \\ -p_{y_i} & p_{x_i} & 0 \end{bmatrix}, \tag{3}$$

by which a cross product $\boldsymbol{p}_i \times \boldsymbol{f}_i$ is expressed as

$$\boldsymbol{p}_i \times \boldsymbol{f}_i = \boldsymbol{S}(\boldsymbol{p}_i)\boldsymbol{f}_i. \tag{4}$$

For the system of the hard-finger grasp, we consider the stiffness effect due to the object rotation $\boldsymbol{\omega} = \zeta\boldsymbol{k}$, where $\boldsymbol{k} \in \mathbb{R}^3$ is the rotation axis and $\zeta \in \mathbb{R}$ is the amount of the rotation. It is assumed that the object is only rotated around the center of mass. It is also assumed that the contact force $\boldsymbol{f}_i$ and the contact point on the object $\boldsymbol{p}_i$ are invariant. This assumption can be realized by an appropriate control method if a joint structure satisfies the *manipulable* condition [14]. We define the *moment stability* as

$$(\zeta\boldsymbol{k})^{\mathrm{T}}\boldsymbol{M}(\zeta,\boldsymbol{k}) < 0 \text{ for any } \boldsymbol{k},\ \zeta, \tag{5}$$

where $\boldsymbol{M}(\zeta,\boldsymbol{k}) := [M_x\ M_y\ M_z]^{\mathrm{T}} \in \mathbb{R}^3$ is the moment caused by the object rotation $\boldsymbol{\omega} = \zeta\boldsymbol{k}$. Eq. (5) is the extension of the 2-dimensional moment stability in [13] and means that $\boldsymbol{M}(\zeta,\boldsymbol{k})$ is the restoring force against the rotational displacement $\boldsymbol{\omega} = \zeta\boldsymbol{k}$ as shown in Fig. 1.

The resultant moment $\boldsymbol{M}(\zeta,\boldsymbol{k})$ of the hard-finger grasp is given by

$$\boldsymbol{M}(\zeta,\boldsymbol{k}) = \sum_{i=1}^{N} (\boldsymbol{R}_k(\zeta)\boldsymbol{p}_i) \times \boldsymbol{f}_i, \tag{6}$$

where $\boldsymbol{R}_k(\zeta) \in \mathbb{R}^{3\times3}$ is the rotation matrix about $\boldsymbol{k}$-axis through ζ defined as [14]

$$\boldsymbol{R}_k(\zeta) = \begin{bmatrix} k_x^2 v_\zeta + c_\zeta & k_x k_y v_\zeta - k_z s_\zeta & k_x k_z v_\zeta + k_y s_\zeta \\ k_x k_y v_\zeta + k_z s_\zeta & k_y^2 v_\zeta + c_\zeta & k_y k_z v_\zeta - k_x s_\zeta \\ k_x k_z v_\zeta - k_y s_\zeta & k_y k_z v_\zeta + k_x s_\zeta & k_z^2 v_\zeta + c_\zeta \end{bmatrix}, \tag{7}$$

where $c_\zeta := \cos\zeta$, $s_\zeta := \sin\zeta$ and $v_\zeta := 1 - \cos\zeta$. It is here assumed that the perturbed rotation amount ζ is small. From the assumption and (3), (7) is linearized as

$$\boldsymbol{R}_k(\zeta) = \begin{bmatrix} 1 & -k_z\zeta & k_y\zeta \\ k_z\zeta & 1 & -k_x\zeta \\ -k_y\zeta & k_x\zeta & 1 \end{bmatrix} = \boldsymbol{I}_3 + \boldsymbol{S}(\zeta\boldsymbol{k}). \tag{8}$$

Substituting (8) into (6), we get

$$\begin{aligned} \boldsymbol{M}(\zeta,\boldsymbol{k}) &= \sum_{i=1}^{N} (\boldsymbol{p}_i + \boldsymbol{S}(\zeta\boldsymbol{k})\boldsymbol{p}_i) \times \boldsymbol{f}_i \\ &= \underbrace{\sum_{i=1}^{N} \boldsymbol{S}(\boldsymbol{p}_i)\boldsymbol{f}_i}_{0} + \sum_{i=1}^{N} \boldsymbol{S}(\boldsymbol{S}(\zeta\boldsymbol{k})\boldsymbol{p}_i)\boldsymbol{f}_i \\ &= -\sum_{i=1}^{N} \left(\boldsymbol{p}_i^{\mathrm{T}}\boldsymbol{f}_i\boldsymbol{I}_3 - \boldsymbol{p}_i\boldsymbol{f}_i^{\mathrm{T}}\right)\zeta\boldsymbol{k}, \end{aligned} \tag{9}$$

where the first term of the second row equals 0 from (2) and the second term is simplified by easy calculation [14]. Substituting (9) into (5) leads to

$$(\zeta\boldsymbol{k})^{\mathrm{T}}\boldsymbol{M}(\zeta,\boldsymbol{k}) = -(\zeta\boldsymbol{k})^{\mathrm{T}}\boldsymbol{K}_h(\zeta\boldsymbol{k}), \tag{10}$$

where

$$\boldsymbol{K}_h := \sum_{i=1}^{N} \boldsymbol{K}_{h_i},\ \boldsymbol{K}_{h_i} := \boldsymbol{p}_i^{\mathrm{T}}\boldsymbol{f}_i\boldsymbol{I}_3 - \boldsymbol{p}_i\boldsymbol{f}_i^{\mathrm{T}}.$$

Since (10) is the quadratic form, the condition to hold the moment stability (5) is given by [16]

$$\bar{\boldsymbol{K}}_h > 0, \tag{11}$$

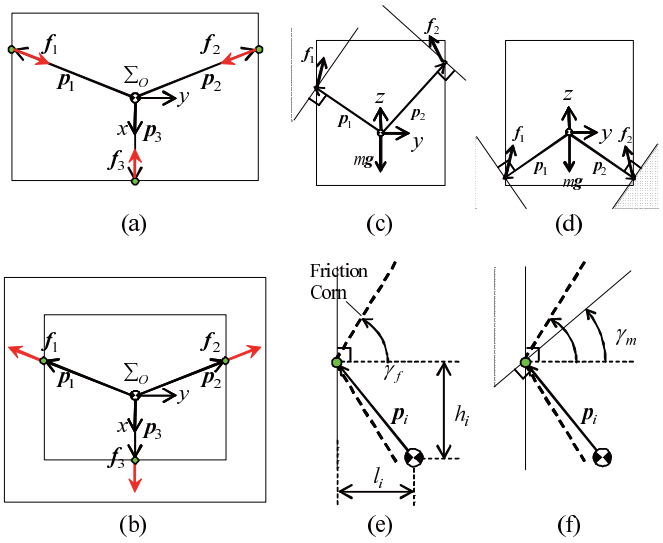

Fig. 2. Grasp situations not to and to satisfy (12).

where

$$\bar{\boldsymbol{K}}_h := \sum_{i=1}^{N} \bar{\boldsymbol{K}}_{h_i},\ \bar{\boldsymbol{K}}_{h_i} := \frac{1}{2}(\boldsymbol{K}_{h_i} + \boldsymbol{K}_{h_i}^{\mathrm{T}}).$$

From Sylvester's criterion [16], The condition to satisfy (11) is

$$\det\bar{\boldsymbol{K}}_h^j > 0,\ j = 1,2,3, \tag{12}$$

where $\bar{\boldsymbol{K}}_h^j \in \mathbb{R}^{j\times j}$ is the jth principal minors of $\bar{\boldsymbol{K}}_h$.

Here, we consider a condition to satisfy the moment stability. The principal minors $\bar{\boldsymbol{K}}_h^j$ are calculated from (10) and (11) as

$$\det\bar{\boldsymbol{K}}_h^1 = \bar{k}_h^{11} \tag{13}$$

$$\det\bar{\boldsymbol{K}}_h^2 = \bar{k}_h^{11}\bar{k}_h^{22} - (\bar{k}_h^{12})^2 \tag{14}$$

$$\det\bar{\boldsymbol{K}}_h^3 = \bar{k}_h^{11}\bar{k}_h^{22}\bar{k}_h^{33} + 2\bar{k}_h^{12}\bar{k}_h^{13}\bar{k}_h^{23} - \bar{k}_h^{11}(\bar{k}_h^{23})^2 - \bar{k}_h^{22}(\bar{k}_h^{12})^2 - \bar{k}_h^{33}(\bar{k}_h^{13})^2, \tag{15}$$

where $\bar{k}_h^{ij}$ is the component of $\bar{\boldsymbol{K}}_h$ at the ith row and jth column given by

$$\bar{k}_h^{11} := \sum_{i=1}^{N}(p_{y_i}f_{y_i} + p_{z_i}f_{z_i}),\ \bar{k}_h^{12} := -\frac{1}{2}\sum_{i=1}^{N}(p_{y_i}f_{x_i} + p_{x_i}f_{y_i})$$

$$\bar{k}_h^{13} := -\frac{1}{2}\sum_{i=1}^{N}(p_{z_i}f_{x_i} + p_{x_i}f_{z_i}),\ \bar{k}_h^{22} := \sum_{i=1}^{N}(p_{x_i}f_{x_i} + p_{z_i}f_{z_i})$$

$$\bar{k}_h^{23} := -\frac{1}{2}\sum_{i=1}^{N}(p_{z_i}f_{y_i} + p_{y_i}f_{z_i}),\ \bar{k}_h^{33} := \sum_{i=1}^{N}(p_{x_i}f_{x_i} + p_{y_i}f_{y_i}) \tag{16}$$

From (13), (14) and (16), the condition to satisfy $\det\bar{\boldsymbol{K}}_h^j > 0$ $(j = 1,2)$ is easily obtained as

$$\bar{k}_h^{11} > 0,\ \bar{k}_h^{22} > 0. \tag{17}$$

Since the condition of (15) depends on a grasp situation, it is considered in an example of Fig. 2 (a), where the following relations hold:

$$\begin{aligned}
&p_{x_i}f_{x_i} + p_{y_i}f_{y_i} < 0\ (i = 1,2,3),\\
&p_{x_1} = p_{x_2} = -2p_{x_3} = p_x < 0,\ f_{x_1} = f_{x_2} = -\frac{1}{2}f_{x_3} = f_x > 0,\\
&p_{y_1} = -p_{y_2} = p_y < 0,\ p_{y_3} = 0,\ f_{y_1} = -f_{y_2} > 0, f_{y_3} = 0,\\
&p_{z_1} = p_{z_2} = p_{z_3} = p_z > 0,\ f_{z_1} = f_{z_2} = f_{z_3} = f_z.
\end{aligned} \tag{18}$$

The gravity direction is in the z-axis. This example is a typical grasp situation where the contact points surround the center of mass (CM) and the grasping forces are in the direction to the CM. From (18), it is easily obtained that $\bar{k}_h^{33} < 0$, $\bar{k}_h^{12} = 0$ and $\bar{k}_h^{13}$. By these facts and (17),

$$\det\bar{\boldsymbol{K}}_h^3 = \bar{k}_h^{11}\left\{\bar{k}_h^{22}\bar{k}_h^{33} - (\bar{k}_h^{23})^2\right\} < 0. \tag{19}$$

Therefore, it is necessary to hold $\bar{k}_h^{33} > 0$ in order to satisfy $\det\bar{\boldsymbol{K}}_h^3 > 0$. This condition is satisfied in the strange grasp situation of a hollow object of Fig. 2 (b), where the grasping forces are in the inverse direct to the CM. Furthermore, it is necessary to satisfy (17). A sufficient condition of (17) is given by

$$p_{y_i}f_{y_i} + p_{z_i}f_{z_i} > 0,\ p_{x_i}f_{x_i} + p_{z_i}f_{z_i} > 0\ (i = 1,2,3). \tag{20}$$

For space limitation, the condition $p_{y_i}f_{y_i} + p_{z_i}f_{z_i} > 0$ is considered. The areas of $\boldsymbol{f}_1$ and $\boldsymbol{f}_2$ to satisfy (20) are represented by the shaded areas in (c) and (d) of Fig. 2. It is obvious that there do not exist $\boldsymbol{f}_1$ and $\boldsymbol{f}_2$ when the contact positions are under the center of mass. In order to construct the grasp of the object, the contact force $\boldsymbol{f}_i$ also has to satisfy the friction condition illustrated in (3) of Fig. 2 (e):

$$\boldsymbol{f}_i^{\mathrm{T}}\boldsymbol{e}_{t_i} \le \mu_i|\boldsymbol{f}_i^{\mathrm{T}}\boldsymbol{e}_{n_i}|, \tag{21}$$

where $\boldsymbol{e}_{n_i}$, $\boldsymbol{e}_{t_i} \in \mathbb{R}^3$ are the normal and tangent vectors and μ_i is the static friction coefficient. Fig. 2 (f) shows the friction cone and the area of (20), where γ_{f_i} and γ_{m_i} are the angles of the boundaries of the friction cone and (20) from the contact normal respectively. These angles are defined as

$$\gamma_{f_i} := \tan^{-1}\mu_i,\quad \gamma_{m_i} := \tan^{-1}\frac{h_i}{l_i}, \tag{22}$$

where l_i and h_i are the distances of the ith contact point from the CM along the normal and tangent respectively. Therefore, it is necessary for the distances l_i and h_i of the contact point to satisfy

$$\gamma_{m_i} \le \gamma_{f_i} \quad\Leftrightarrow\quad \frac{h_i}{l_i} \le \mu_i \tag{23}$$

as shown in (f) of Fig. 2.

Remark 1: From (23), it is easy to grasp a slender object with the upper contact points while it is difficult to grasp a wide object with central contact points. In other words, the contact locations for the stability are restricted to far upper from the CM. Furthermore, Fig. 2 (b) implies that kinds of object shape to satisfy the moment stability are restricted to hollow objects. These results indicate that it is impossible to realize the moment stability by hard-fingers.

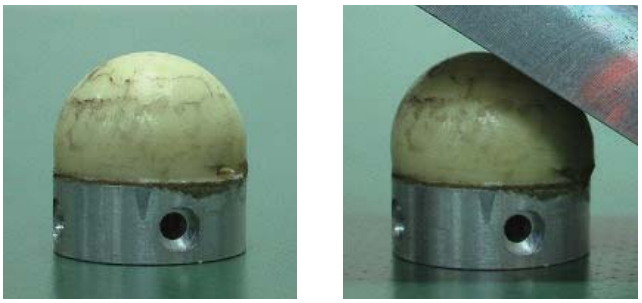

Fig. 3. Soft finger and Contact situation.

III. Stability Analysis of Soft-Finger Grasp

In this section, we secondly analyze stability of an object grasped by a pair of soft-fingers in 3D space. A deformation model of a soft-finger and a contact kinematics are necessary for the analysis. We use a 3-dimensional deformation model and the rolling contact with deformation as a contact kinematics, which are proposed in [15].

A. 3-Dimensional Deformation Model

In this paper, a soft-finger means a semispherical soft material, the flat part of which is attached to a rigid base as in the left figure of Fig. 3. We make a deformation model of a soft-finger with a contact to a plane of a polyhedral object as shown in the right of Fig. 3.

The frame and coordinates of the configuration of the contact point is defined here. The finger frame Σ_{F_i} is attached to the center of the soft-finger as in the left of Fig. 4 (a). The y_{F_i}- and z_{F_i}-axes are in the finger base and the x_{F_i}-axis goes through the finger. Since the soft-finger is a semisphere, the contact point on the soft-fingertip before deformation is expressed by the polar coordinates (θ_i, ϕ_i, r_i), where θ_i, ϕ_i and r_i are the angles and radius. When the finger is deformed with the contact on the object, the contact surface is the circle from the geometry of the finger and object as shown in the left figure of Fig. 4 (a). Therefore, the contact point after deformation is defined as the center of the contact surface. The right of Fig. 4 (a) shows the cross section along the longitude through the contact point of the left figure. The deformed area overlapping the object is expressed by the compressive deformation displacement $\delta_{r_i} \in \mathbb{R}_+$ in the radial direction. As shown in the left of Fig. 4 (b), the deformations along the finger surface are expressed by the shearing and compressive deformation angles $\delta_{\theta_i},\ \delta_{\phi_i} \in \mathbb{R}$ in the inverse directions of (θ_i, ϕ_i). In the right of Fig. 4 (b), the contact frame $\Sigma_{C_{F_i}}$ is attached at the contact point, which is defined such that the $x_{C_{F_i}}$- and $y_{C_{F_i}}$-axes are in the longitude and latitude through the contact point and the $z_{C_{F_i}}$-axis is in the normal to the finger surface. The torsion deformation with respect to the contact surface is expressed by the shearing deformation angle δ_{ϕ_i} about the $z_{C_{F_i}}$-axis in the inverse direction. Define the deformation coordinates as $\boldsymbol{\delta}_i := [\delta_{r_i} \quad \delta_{\theta_i} \quad \delta_{\phi_i} \quad \delta_{\psi_i}]^{\mathrm{T}} \in \mathbb{R}^4$.

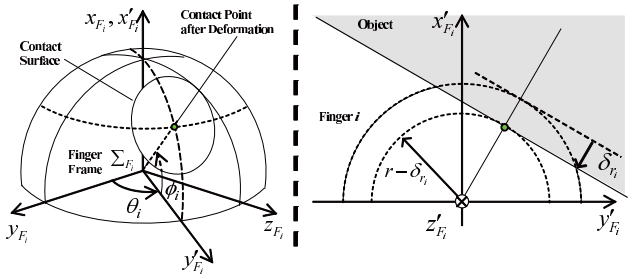

(a) Polar coordinates and radius coordinate δ_{r_i}

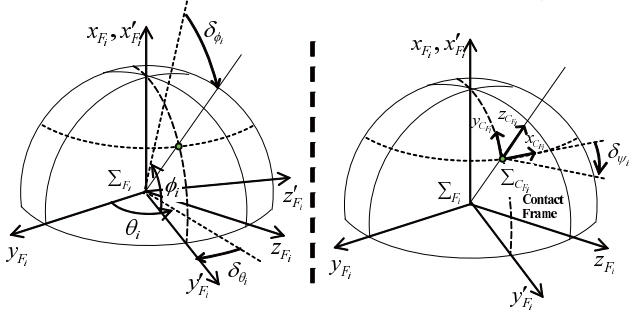

(b) Spherical and torsion coordinates $(\delta_{\theta_i}, \delta_{\phi_i}), \delta_{\psi_i}$

Fig. 4. The coordinates of the deformation of the soft-finger.

From Hook's law, the forces produced by the deformations are derived as the functions of the deformations $\boldsymbol{\delta}_i$:

$$
\begin{aligned}
F_{r_i}(\delta_{r_i}) &= k_{r_i}\pi\delta_{r_i}^2 \\
M_{\theta_i}(\delta_{\theta_i}, \phi_i) &= \frac{1}{10}k_{\theta_i}\pi r_i^4\left\{1 + c_{\phi_i}(1 + c_{\phi_i})(1 + c_{\phi_i}^2)\right\}\delta_{\theta_i} \\
M_{\phi_i}(\delta_{\phi_i}, \phi_i) &= \frac{2}{3}k_{\phi_i}r_i^3\left(\frac{1}{\pi - \phi_i} + \frac{1}{\phi_i}\right)\delta_{\phi_i} \\
M_{\psi_i}(\delta_{r_i}, \delta_{\psi_i}) &= \frac{1}{10}k_{\psi_i}\pi\left\{r_i^2 - (r_i - \delta_{r_i})^2\right\}^2\delta_{\psi_i}. \qquad (24)
\end{aligned}
$$

F_{r_i} is the force in the radial direction and M_{θ_i} and M_{ϕ_i} are the moments about the x'_{F_i}- and z'_{F_i}- axes in the left figure of Fig. 4 (b) where $c_{\phi_i} := \cos\phi_i$. M_{ψ_i} is the moment about the $z_{C_{F_i}}$-axis in the right figure of Fig. 4 (b).

B. Rolling Contact with Deformation

Let us denote the variables to express the contact configuration *without the deformation* in order to consider the rolling contact. Fig. 5 represents the neighborhood of the ith contact. $\Sigma_{C_{F_i}}$ and $\Sigma_{C_{O_i}}$ are the coordinate frames attached on the surfaces of the ith finger and the object with the origins at the ith contact point. The z_{F_i}- and z_i-axes of the frames are outward and normal to the surfaces of the

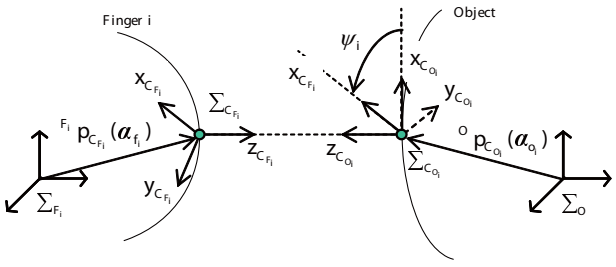

Fig. 5. Contact coordinates before the deformation.

ith finger and the object, respectively. The contact point in the finger surface is represented by the position vector ${}^{F_i}\boldsymbol{p}_{C_{F_i}}(\theta_i, \phi_i) \in \mathbb{R}^3$. Similarly, the contact point on the object surface is represented by ${}^{O}\boldsymbol{p}_{C_{O_i}}(x_{o_i}, y_{o_i}) \in \mathbb{R}^3$. Note that (θ_i, ϕ_i), i.e., the some of the previous polar coordinates of the soft-finger, and (x_{o_i}, y_{o_i}) are the 2D local coordinates on the finger and object surfaces in x- and y-axes of $\Sigma_{C_{F_i}}$ and $\Sigma_{C_{O_i}}$. In addition, since x- and y-axes of $\Sigma_{C_{F_i}}$ and $\Sigma_{C_{O_i}}$ are in the same contact tangent surface, let ψ_i be the angle between the x- axes of $\Sigma_{C_{F_i}}$ and $\Sigma_{C_{O_i}}$ *without the torsion deformation* δ_{ψ_i} as shown in Fig. 5. Then, the configuration of the contact points is described by the contact coordinates $\boldsymbol{\eta}_i := (\theta_i, \phi_i, x_{o_i}, y_{o_i}, \psi_i)$ [14].

Considering the deformations $\boldsymbol{\delta}_i$ into the contact coordinates $\boldsymbol{\eta}_i$, the contact point ${}^{F_i}\boldsymbol{p}_{C_{F_i}}$ *after the deformation* and the contact frame $\boldsymbol{R}_{FC_{F_i}}$ are expressed as

$$ {}^{F_i}\boldsymbol{p}_{C_{F_i}} = \begin{bmatrix} R_i s_{\Phi_i} \\ R_i c_{\Theta_i} c_{\Phi_i} \\ R_i s_{\Theta_i} c_{\Phi_i} \end{bmatrix}, \boldsymbol{R}_{F_i C_{F_i}} = \begin{bmatrix} 0 & c_{\Phi_i} & s_{Phi_i} \\ -s_{\Theta_i} & -s_{\Phi_i} c_{\Theta_i} & c_{\Theta_i} c_{\Phi_i} \\ c_{\Theta_i} & -s_{\Phi_i} s_{\Theta_i} & s_{\Theta_i} c_{\Phi_i} \end{bmatrix} \tag{25} $$

where $c_{\Theta_i} = \cos\Theta_i$, $s_{\Theta_i} = \sin\Theta_i$, $c_{\Phi_i} = \cos\Phi_i$, $s_{\Phi_i} = \sin\Phi_i$,

$$ R_i := r_i - \delta_{r_i}, \ \Theta_i := \theta_i - \delta_{\theta_i}, \ \Phi_i := \phi_i - \delta_{\phi_i}. \tag{26} $$

In this paper, we consider the pure rolling contact [14]. The pure rolling contact means that the finger does not slip on the object without rotationally slipping around the $z_{C_{F_i}}$-axis. The relationship between the contact coordinates is given by [15]

$$ \begin{bmatrix} dx_{o_i} \\ dy_{o_i} \end{bmatrix} = \underbrace{\begin{bmatrix} \cos\Psi_i & -\sin\Psi_i \\ -\sin\Psi_i & -\cos\Psi_i \end{bmatrix}}_{\boldsymbol{R}_{\psi_i}} \underbrace{\begin{bmatrix} R_i \cos\Phi_i & 0 \\ 0 & R_i \end{bmatrix}}_{\boldsymbol{M}_{gf_i}} \begin{bmatrix} d\theta_i \\ d\phi_i \end{bmatrix} \tag{27} $$

$$ d\psi_i = d\theta_i \sin\Phi_i, \tag{28} $$

where $(d\theta_i, d\phi_i)$, (dx_{o_i}, dy_{o_i}) and $d\psi_i$ are the small displacements of the contact coordinates and

$$ \Psi_i := \psi_i + \delta_{\psi_i}. \tag{29} $$

(27) means that the contact displacements of the finger and object on the contact surface equal to each other. $\boldsymbol{R}_{\psi_i}$ is the rotation matrix between the (x, y) coordinates of $\Sigma_{C_{F_i}}$ and $\Sigma_{C_{O_i}}$. $\boldsymbol{M}_{gf_i}$ translates the angle displacements to the linear ones. (28) means that the angle displacements in the $z_{C_{F_i}}$ due to ψ_i and θ_i around the x_{F_i}-axis equal to each other because the angle between the $z_{C_{F_i}}$- and x_{F_i}-axes is $\pi - \Phi_i$.

Remark 2: Note that there do not exist the small displacements of the deformations $\boldsymbol{\delta}_i$ in the rolling contact equations of (27) and (28). This is because the deformations $\boldsymbol{\delta}_i$ do not include the displacements on the finger surface and can denote only the shift of the contact point expressed in $\Sigma_{C_{F_i}}$ due to the deformed soft-finger.

C. Derivation of Moment due to Object Rotation

The problem setting is mentioned for preliminary. The left of Fig. 6 shows an object grasped by the soft-fingers. The object is assumed to be a convex polyhedron. $\boldsymbol{F}_{C_i} \in \mathbb{R}^3$ and

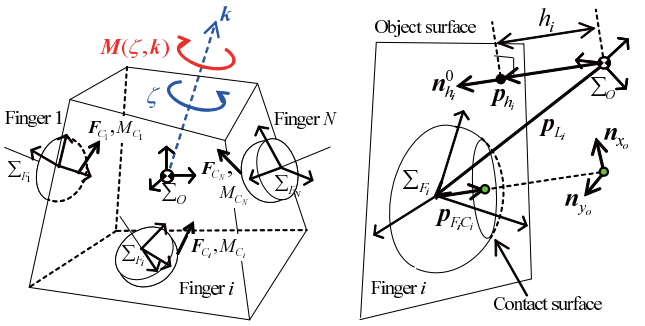

Fig. 6. An object grasped by soft-fingers.

$M_{C_i} \in \mathbb{R}$ are the contact force and moment expressed in $\Sigma_{C_{F_i}}$ and they satisfy the following equilibrium equations:

$$ \sum_{i=N}^{N} \boldsymbol{R}_{OC_{F_i}} \boldsymbol{F}_{C_i} = \boldsymbol{0}, \tag{30} $$

$$ \sum_{i=1}^{N} \left(\boldsymbol{S}(\boldsymbol{p}_i) \boldsymbol{R}_{OC_{F_i}} \boldsymbol{F}_{C_i} + M_{C_i} \boldsymbol{R}_{OC_{F_i}} \boldsymbol{e}_z \right) = \boldsymbol{0}, \tag{31} $$

where $\boldsymbol{e}_z := [0 \ 0 \ 1]^{\mathrm{T}}$, $\boldsymbol{R}_{OC_{F_i}} := \boldsymbol{R}(\boldsymbol{\theta}_{F_i}) \boldsymbol{R}_{F_i C_{F_i}}$, $\boldsymbol{R}(\boldsymbol{\theta}_{F_i})$ is the rotation matrix from Σ_{F_i} to Σ_O. $\boldsymbol{F}_{C_i}$ and M_{C_i} are expressed by the deformation forces and moment of (24) as

$$ F^x_{C_i} = \frac{M_{\theta_i} - M_{\psi_i} \sin\Phi_i}{R_i \cos\Phi_i}, F^y_{C_i} = \frac{F_{\phi_i}}{R_i}, F^z_{C_i} = F_{r_i}, M^z_{C_i} = M_{\psi_i}. \tag{32} $$

In the right figure, $\boldsymbol{p}_{L_i} \in \mathbb{R}^3$ is the center of the finger and $\boldsymbol{p}_{F_i C_i} \in \mathbb{R}^3$ is the vector from the center of the finger to the contact point expressed in Σ_O. Therefore, the contact point $\boldsymbol{p}_i$ is given by

$$ \boldsymbol{p}_i = \boldsymbol{p}_{L_i} + \boldsymbol{p}_{F_i C_{F_i}}, \ \boldsymbol{p}_{F_i C_{F_i}} := \boldsymbol{R}_{F_i} {}^{F_i}\boldsymbol{p}_{C_{F_i}}. \tag{33} $$

$\boldsymbol{p}_{h_i} \in \mathbb{R}^3$ is the point with the minimum distance h_i of the object surface from the CM and $\boldsymbol{n}^0_{h_i} \in \mathbb{R}^3$ is the normal to the object surface in the initial situation. $\boldsymbol{n}_{x_{o_i}}, \boldsymbol{n}_{y_{o_i}} \in \mathbb{R}^3$ are the unit vectors to express the x- and y-axes of $\Sigma_{C_{O_i}}$.

We consider the moment produced by the soft-fingers when the object is rotated about $\boldsymbol{k}$-axis through ζ from the equilibrium conditions (30) and (31). Because the contact force and moment $(\boldsymbol{F}_{C_i}, M_{C_i})$ and the contact point $\boldsymbol{p}_i$ obviously depend on them from (24), (32), (33) and (25), it is necessary to obtain the changed contact coordinates $\boldsymbol{\eta}_i(\zeta)$ and the deformation $\boldsymbol{\delta}_i(\zeta)$ due to the rotation $(\zeta, \boldsymbol{k})$:

$$ \begin{aligned} \theta_i(\zeta) &:= \theta^0_i + \Delta\theta_i(\zeta), \ \phi_i(\zeta) := \phi^0_i + \Delta\phi_i(\zeta) \\ x_{o_i}(\zeta) &:= x^0_{o_i} + \Delta x_{o_i}(\zeta), \ y_{o_i}(\zeta) := y^0_{o_i} + \Delta y_{o_i}(\zeta) \\ \psi_i(\zeta) &:= \psi^0_i + \Delta\psi_i(\zeta) \\ \delta_{\theta_i}(\zeta) &:= \delta^0_{\theta_i} + \Delta\delta_{\theta_i}(\zeta), \ \delta_{\phi_i}(\zeta) := \delta^0_{\phi_i} + \Delta\delta_{\phi_i}(\zeta) \\ \delta_{\psi_i}(\zeta) &:= \delta^0_{\psi_i} + \Delta\delta\psi_i(\zeta), \end{aligned} \tag{34} $$

where the variables with the superscript 0 are the initial variables satisfying the initial equilibrium equations of (30) and (31), and the ones with the Δ is the increments from the grasping equilibrium due to the rotation $(\zeta, \boldsymbol{k})$. The scheme to obtain $\boldsymbol{\eta}_i$ and $\boldsymbol{\delta}_i$ is shown in the following:

1) To obtain $\delta_{r_i}(\zeta)$ and $(\Delta x_{o_i}(\zeta), \Delta y_{o_i}(\zeta))$ from the geometric viewpoint.

2) To obtain $(\Theta_i(\zeta), \Phi_i(\zeta))$ and $\Psi_i(\zeta)$ from the geometric viewpoint.
3) To obtain $(\Delta\theta_i(\zeta), \Delta\phi_i(\zeta))$ and $\Delta\psi_i(\zeta)$ by solving the rolling contact equations (27) and (28) with the obtained $\Phi_i(\zeta)$ and $\Psi_i(\zeta)$.
4) To obtain $(\Delta\delta_{\theta_i}(\zeta), \Delta\delta_{\phi_i}(\zeta))$ and $\Delta\delta_{\psi_i}(\zeta)$ by (26) and (29) with the obtained $(\Theta_i(\zeta), \Phi_i(\zeta))$ and $\Psi_i(\zeta)$ and $(\Delta\theta_i(\zeta), \Delta\phi_i(\zeta))$.

1) Derivation of $\delta_{r_i}(\zeta)$ and $(\Delta x_{o_i}(\zeta), \Delta y_{o_i}(\zeta))$: Since the contact surface equals to the object surface as seen in Fig. 6, the vector $\boldsymbol{p}_{F_iC_{F_i}}$ is in the same direction of $\boldsymbol{p}_{h_i}$ given by

$$\boldsymbol{p}_{h_i}(\zeta) = \boldsymbol{R}_k(\zeta)(h_i \boldsymbol{n}^0_{h_i}) = h_i \boldsymbol{n}_{h_i}(\zeta),\ \boldsymbol{n}_{h_i}(\zeta) := \boldsymbol{R}_k(\zeta)\boldsymbol{n}^0_{h_i}. \tag{35}$$

Therefore, by considering the distance between the center of the finger and the CM in the direction of $\boldsymbol{p}_{h_i}$, the magnitude $R_i(\zeta)$ of $\boldsymbol{p}_{F_iC_{F_i}}$ is given by

$$R_i(\zeta) = L_{h_i}(\zeta) - h_i,\ L_{h_i}(\zeta) := \boldsymbol{n}^{\mathrm{T}}_{h_i}(\zeta)\boldsymbol{p}_{L_i}, \tag{36}$$

where $L_{h_i}(\zeta) \in \mathbb{R}$ is the distance between the center of the finger and the CM in the direction of $\boldsymbol{p}_{h_i}$. From (26), $\delta_{r_i}(\zeta)$ is obtained as

$$\delta_{r_i}(\zeta) = r_i + h_i - L_{h_i}(\zeta). \tag{37}$$

Next, from $\boldsymbol{p}_{F_iC_{F_i}} = -R_i(\zeta)\boldsymbol{n}_{h_i}(\zeta)$, (33) and (35), the contact point $\boldsymbol{p}_i$ expressed on the object surface with $\zeta = 0$ is given by

$$\boldsymbol{p}^0_i(\zeta) = \boldsymbol{R}^{\mathrm{T}}_k(\zeta)\boldsymbol{p}_{L_i} - R_i(\zeta)\boldsymbol{n}^0_{h_i}. \tag{38}$$

Therefore, $(\Delta x_{o_i}(\zeta), \Delta y_{o_i}(\zeta))$ are obtained as

$$\Delta x_{o_i}(\zeta) = (\boldsymbol{n}^0_{x_i})^{\mathrm{T}}\Delta\boldsymbol{p}^0_i(\zeta), \Delta y_{o_i}(\zeta) = (\boldsymbol{n}^0_{y_i})^{\mathrm{T}}\Delta\boldsymbol{p}^0_i(\zeta), \tag{39}$$

where $\Delta\boldsymbol{p}^0_i(\zeta) := \boldsymbol{p}^0_i(\zeta) - \boldsymbol{p}^0_i$ and $\boldsymbol{p}^0_i$ is the initial state.

2) Derivation of $(\Theta_i(\zeta), \Phi_i(\zeta))$ and $\Psi_i(\zeta)$: Substituting $\boldsymbol{p}_{F_iC_{F_i}} = -R_i(\zeta)\boldsymbol{n}_{h_i}(\zeta)$ and (25) into (33) yield

$$\begin{bmatrix} \sin\Phi_i(\zeta) \\ \cos\Theta_i(\zeta)\cos\Phi_i(\zeta) \\ \sin\Theta_i(\zeta)\cos\Phi_i(\zeta) \end{bmatrix} = \begin{bmatrix} \alpha_i(\zeta) \\ \beta_i(\zeta) \\ \gamma_i(\zeta) \end{bmatrix} := \boldsymbol{R}^{\mathrm{T}}_{F_i}(\boldsymbol{\theta}_{F_i})\boldsymbol{n}_{h_i}(\zeta). \tag{40}$$

From (40), $(\Theta_i(\zeta), \Phi_i(\zeta))$ are obtained as

$$\Phi_i(\zeta) = \sin^{-1}\alpha_i(\zeta),\ \Theta_i(\zeta) = \sin^{-1}\left(\frac{\gamma_i(\zeta)}{\cos\Phi_i(\zeta)}\right). \tag{41}$$

From Fig. 5, $\Psi_i(\zeta)$ is the angle between the $x_{C_{F_i}}$- and $x_{C_{O_i}}$-axes defined by the following corresponding unit vectors:

$$\boldsymbol{n}_{x_{C_{F_i}}} := \begin{bmatrix} 0 \\ -\sin\Theta_i(\zeta) \\ \cos\Theta_i(\zeta) \end{bmatrix},\ \boldsymbol{n}_{x_{C_{O_i}}} := \boldsymbol{R}_k(\zeta)\boldsymbol{n}^0_{x_{o_i}}, \tag{42}$$

where $\boldsymbol{n}_{x_{C_{F_i}}}$ is the first column of $\boldsymbol{R}_{F_iC_{F_i}}$ of (25). Considering the sign of $\Psi_i(\zeta)$ which equals the sign of $\psi_i(\zeta)$, we obtain the following $\Psi_i(\zeta)$:

$$\Psi_i(\zeta) = a_{\Psi_i}\cos^{-1}\left((\boldsymbol{n}_{x_{C_{F_i}}})^{\mathrm{T}}\boldsymbol{n}_{x_{C_{O_i}}}\right), \tag{43}$$

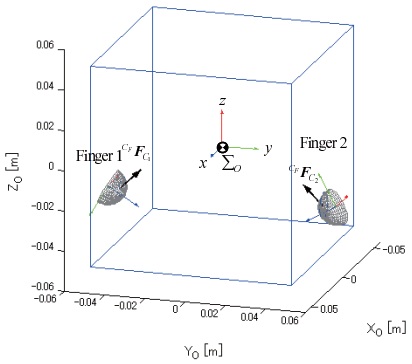

Fig. 7. A rectangular object grasped by two soft-fingers.

where

$$a_{\Psi_i} := \mathrm{sign}\left\{(\boldsymbol{n}_{x_{C_{F_i}}} \times \boldsymbol{n}_{x_{C_{O_i}}})^{\mathrm{T}}\boldsymbol{p}_{F_iC_{F_i}}\right\}.$$

3) Derivation of $(\Delta\theta_i(\zeta), \Delta\phi_i(\zeta))$ and $\Delta\psi_i(\zeta)$: From the pure rolling equations (27) and (28), $(\Delta\theta_i(\zeta), \Delta\phi_i(\zeta))$ and $\Delta\psi_i(\zeta)$ are given by

$$\begin{bmatrix} \Delta\theta_i(\zeta) \\ \Delta\phi_i(\zeta) \end{bmatrix} = \int_0^\zeta \boldsymbol{M}^{-1}_{gf_i}(\tilde{\zeta})\boldsymbol{R}^{\mathrm{T}}_{\psi_i}(\tilde{\zeta}) \begin{bmatrix} \frac{d(\Delta x_{o_i}(\tilde{\zeta}))}{d\tilde{\zeta}} \\ \frac{d(\Delta y_{o_i}(\tilde{\zeta}))}{d\tilde{\zeta}} \end{bmatrix} d\tilde{\zeta} \tag{44}$$

$$\Delta\psi_i(\zeta) = \int_0^\zeta \frac{d(\Delta\theta_i(\tilde{\zeta}))}{d\tilde{\zeta}}\sin\Phi_i(\tilde{\zeta})d\tilde{\zeta}. \tag{45}$$

It is difficult to obtain $(\Delta\theta_i(\zeta), \Delta\phi_i(\zeta))$ and $\Delta\psi_i(\zeta)$ as functions of ζ by integrating (44) and (45) analytically because the obtained analytical functions of $R_i(\zeta)$, $\Theta_i(\zeta)$ and $\Psi_i(\zeta)$ are complex. Therefore, $(\Delta\theta_i(\zeta), \Delta\phi_i(\zeta))$ and $\Delta\psi_i(\zeta)$ are obtained numerically in this paper.

4) Derivation of $(\Delta\delta_{\theta_i}(\zeta), \Delta\delta_{\phi_i}(\zeta))$ and $\Delta\delta_{\psi_i}(\zeta)$: From (26), (29) and (34), $(\Delta\delta_{\theta_i}(\zeta), \Delta\delta_{\phi_i}(\zeta))$ and $\Delta\delta_{\psi_i}(\zeta)$ are obtained as

$$\begin{aligned} \Delta\delta_{\theta_i}(\zeta) &= -\Theta_i(\zeta) + \Delta\theta_i(\zeta) + (\theta^0_i - \delta^0_{\theta_i}) \\ \Delta\delta_{\phi_i}(\zeta) &= -\Phi_i(\zeta) + \Delta\phi_i(\zeta) + (\phi^0_i - \delta^0_{\phi_i}) \\ \Delta\delta_{\psi_i}(\zeta) &= \Psi_i(\zeta) - \Delta\psi_i(\zeta) - (\psi^0_i + \delta^0_{\psi_i}). \end{aligned} \tag{46}$$

IV. Numerical Example and Discussion

A Numerical example is shown to confirm the moment stability of the soft-finger grasp.

Fig. 7 shows the case where the rectangular object is grasped at the lower contact points. The radius of the finger is $r_i = 10$[mm] and the stiffness coefficients are $k_{r_i} = 0.377$, $k_{\phi_i} = 0.166$[N/mm^2], $k_{\theta_i} = 0.0266$, $k_{\psi_i} = 0.0488$[N/mm^3] [15]. The height, width, depth and mass of the object are 100[mm] and $m = 1.0$[kg] respectively. The initial contact points are $\boldsymbol{p}^0_1 = (0, -50, -25)$, $\boldsymbol{p}^0_2 = (0, 50, -25)$[mm]. The contact angles are $\theta^0_1 = \theta^0_2 = 0$[deg], $\phi^0_1 = 131$, $\phi^0_2 = 49$[deg]. The initial deformations are $\delta^0_{r_1} = \delta^0_{r_2} = 2.1$[mm], $\delta^0_{\theta_1} = -\delta^0_{\theta_2} = 0$[deg], $\delta^0_{\phi_1} = -\delta^0_{\phi_2} = 11$[deg], $\delta^0_{\psi_1} = \delta^0_{\psi_2} = 0$[deg]. The rotation axis and angles are $\boldsymbol{k} = 1/\sqrt{3}[1\ 1\ 1]^{\mathrm{T}}$ and $\zeta = \pm 2$[deg], which generates the rotation with respect to the all axes.

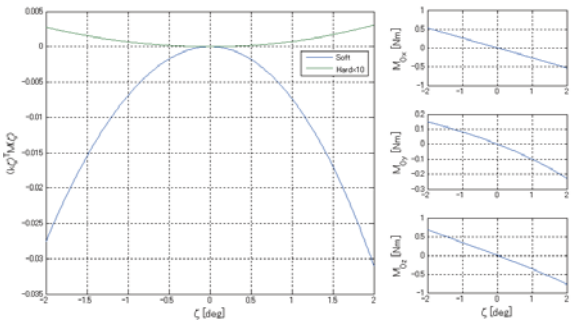

Fig. 8. Simulation result.

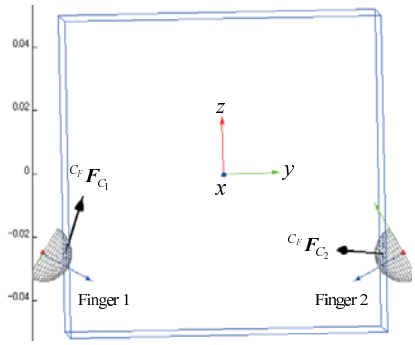

Fig. 9. Simulation result seen from the x-axis rotation.

Fig. 8 shows the simulation result. The left figure shows the inner product between the rotation axis $\zeta \boldsymbol{k}$ and the resultant moment $\boldsymbol{M}(\zeta, \boldsymbol{k})$. It is confirmed that the moment stability is satisfied. Furthermore, the right figure shows the moments with respect to all the (x, y, z)-axes. It is confirmed that the signs of the moments are inverse with respect to the rotation directions. When the two moments are not the restoring moments, the moment stability could hold if the last moment is the restoring one and its effect is much bigger than the effects of the others. However, the stability of its case may reduce. Figs. 9–11 show the results seen from the x-, y- and z-axes respectively, where the the deformation contact forces are illustrated as the solid sick black arrows. In the each figure, it is confirmed that the resultant moment due to the deformation contact force with respect to the corresponding axis is the restoring moment.

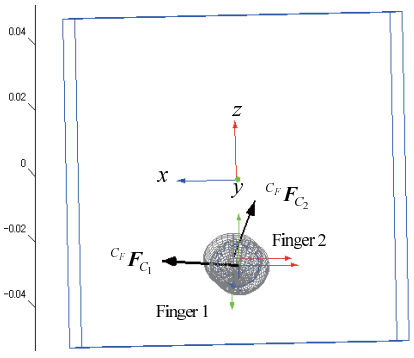

Fig. 10. Simulation result seen from the y-axis rotation.

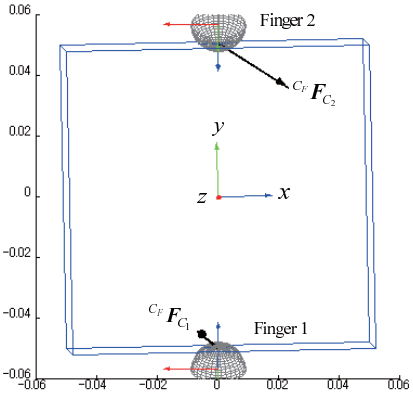

Fig. 11. Simulation result seen from the z-axis rotation.

Remark 3: The torsion moments of the soft-fingers effect on the moment about the y-axis, which have been expected to be the effective restoring moments, e.g., in [8], [14]. Since this effect may be difficult to be illustrated in Fig. 10, the contact moments are shown in Fig. 12 in order to check its effect. Note that the contact moments effect the y-axis. The sum of the contact moments is not the restoring moment because it is positive when $\zeta > 0$. This fact imply that the torsion moments may not effective to the moment stability while its is effective to the force-closure.

Let us consider its reason. The change of the torsion deformation $\Delta\delta_{\psi_i}$ is effected on by Ψ_i and $\Delta\psi_i$ from (46), which are *the terms to reduce each other*. The changes are illustrated in Fig. 13, where the upper and lower figures show the the changes on the first finger-tip and the left side of the object respectively when the object is rotated from $\zeta = 0$ to 2 [deg]. The bule and red arrows represent the $x_{C_{F_1}}$- and $y_{C_{F_1}}$- axes of $\Sigma_{C_{F_1}}$ at the contact point on the finger. The solid sick bule lines represent the shifts of the contact point on the finger-tip surface due to the object rotation and the rolling contact. The black and red circles represent the first and end of the shifts of $\zeta = 0, 2$ [deg]. In the upper figure, the changes $\Delta\Psi_1$ and $\Delta\psi_1$ are shown as the changes of the $x_{C_{F_1}}$-axes. $\Delta\Psi_1$ is directly caused by the relative motion of the finger and object from (43) and very small becuase of small object rotation ζ. On the other hand, $\Delta\psi_1$ is caused by the rolling contact from (45). Note that the shift due to the rolling contact is equal to the shift on the object surface in the lower figure, and is relatively bigger than the shift due the object rotation. *This implies that* $\Delta\psi_1$ *has the dominant effect on the change of the torsion deformation* $\Delta\delta_{\psi_1}$. Furthermore, $\Delta\psi_1$ is caused by the object rotation about the z_O-axis becuse it depends on the change $\Delta\theta_1$ while

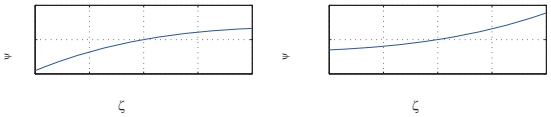

Fig. 12. The contact moments expressed in Σ_O.

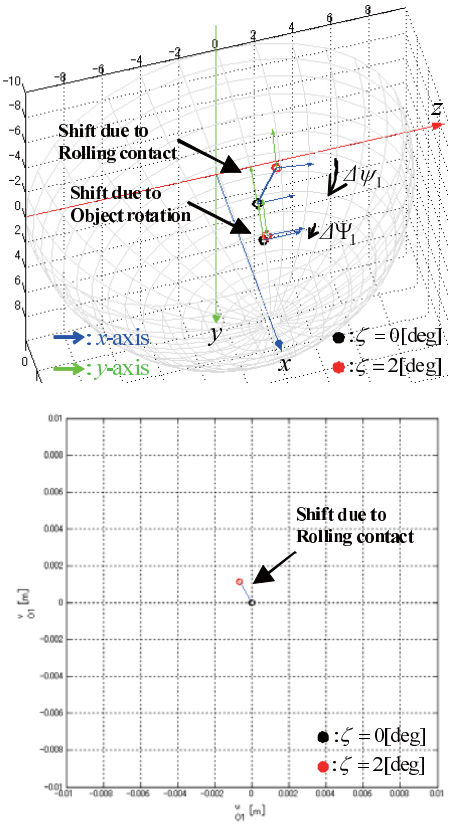

Fig. 13. The changes of the contact configurations on the 1st finger and the object.

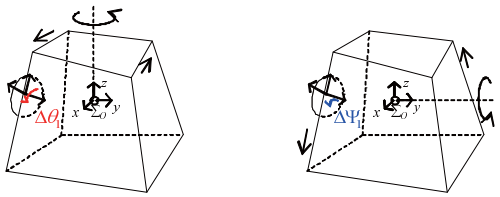

Fig. 14. The illustrations of the changes $\Delta\theta_1$ and $\Delta\Psi_1$.

$\Delta\Psi_1$ is caused by the object rotaion about the y_O-axis as shown in Fig. 14. *Therefore, the moment about the y_O-axis due to the torsion deformation can not effect on the restoring moment when the object is rotated about the z_O-axis.* In that grasp situation, it is necessary to add the third soft-finger which has to produce the inverse moment against the sign of ζ about the y-axis. A example of its contact position of the third finger is in the surfaces perpendicular to the x-axis.

V. Conclusions and Future Works

This paper analyzed stability of an object grasped by soft-fingers in 3-dimensional space based on moment stability. In the case of the hard-finger grasp, we indicated that contact points to satisfy the condition were restricted to upper locations of the center of mass and the class of the object shape was only a kind of hollow objects. In the case of the soft-finger grasp, the consideration showed a novel result that two-fingered grasp could satisfy the moment stability with only two fingers while the hard-fingers needed at least three numbers for the force-closure and could not satisfy the moment stability. On the other hand, it was indicated that the torsion moments did not effect on the moment stability well and it was necessary to add the third finger in a condition of the contact points.

In the case of the dynamics, there are some different points from the static analysis in this paper. Since the rolling relationships of (44) and (45) does not hold becuase of its kinematic forms, it is necessary to consider the acceralation form. Furthremore, it is ncessary to consider an appropriate control method to satisfy the moment stability, an example of which is shown in [15]. A very simple method is the PID control of the finger-tips rigidly. This idea is based on the static analysis in this paper because the finger-tips are assumed to be fixed. The method would utilize the elastic property to satisfy the moment stability.

In future works, it is necessary to consider the friction condition and the limitation of finger joints. We will try to optimize the soft-finger grasp with respect to the mentioned conditions.

References

[1] M. T. Mason and J. K. Salisbury, *Robot Hands and the Mechanics of Manipulation*, Cambridge, MA: MIT Press, 1985.
[2] M. Cutkosky and I. Kao: Computing and Controlling the Compliance of a Robot Hand, *IEEE Trans. Robot. Automat.*, Vol. 5, No. 2, pp. 151-165, 1989.
[3] D. J. Montana: Contact Stability for Two-Fingered Grasps, *IEEE Trans. Robot. Automat.*, Vol. 8, No. 4, pp. 421-430, 1992.
[4] H. Maekawa, K. Tanie and K. Komoriya, Kinematics, Statics and Stiffness Effect of 3D Grasp by Multifingered Hand with Rolling Contact at the Fingertip, Proc. of Int. Conf. on Robot. Automat., pp. 78-85, 1997.
[5] M. Kaneko, N. Imamura, K. Yokoi and K. Tanie, A Realization of Stable Grasp Based on Virtual Stiffness Model by Robot Fingers, IEEE Int. Workshop on Advanced Motion Control, pp.156–163, 1990.
[6] H. Maekawa, K. Tanie, K. Komoriya and M. Kaneko, Stable Grasp and Manipulation of an Object by a Three-Fingered Hand Using Position and Stiffness Control, Proc. of Int. Conf. on Robot. Automat., 1995.
[7] Y. Funahashi, T. Yamada, M. Tate and Y. Suzuki, Grasp stability analysis considering the curvatures at contact points, Proc. Int. Conf. Robot. Automat., pp. 3040–3046, 1996.
[8] K. B. Shimoga and A. A. Goldenberg: Soft Robotic Fingertips Part I: A Comparison of Construction Materials, *Int. J. Robot. Res.*, Vol. 15, No. 4, 320-334, 1996.
[9] T. Inoue and S. Hirai, "Elastic Model of Deformable Fingertip for Soft-fingered Manipulation," *IEEE Trans. on Robotics*, vol. 22, no. 6, pp. 1273–1279, 2006.
[10] T. Inoue and S. Hirai, Quasi-Static Manipulation with Hemispherical Soft Fingertip via Two Rotational Fingers, Proc. Int. Conf. on Robot. Automat., pp.1947–1952, 2005.
[11] T. Inoue and S. Hirai, Study on Hemispherical Soft-Fingered Handling for Fine Manipulation by Minimum D.O.F. Robotic Hand, Proc. Int. Conf. on Robot. Automat., pp.2454–2459, 2006
[12] T. Inoue and S. Hirai, Dynamic Stable Manipulation via Soft-Fingered Hand, Proc. Int. Conf. on Robot. Automat., pp.586-591, 2007.
[13] A. Nakashima, L. Jingtai and Y. Hayakawa, "Stability Analysis of Grasped Object by Soft-Fingers based on Moment Stability," Proc. Int. Conf. 47th CDC, pp.4582-4589, 2008.
[14] R. M. Murray, Z. Li and S. S. Sastry, *A Mathematical Introduction to ROBOTIC MANIPULATION*, CRC Press, 1994.
[15] A. Nakashima, T. Shibata and Y. Hayakawa, "Grasp and Manipulation by Soft-Finger with 3-Dimensional Deformation," SICE Journal of Control, Measurement and System Integration, Vol. 2, No. 2, pp. 78–87, 2009.
[16] S. MacLane and G. Birkoff, *ALGEBRA*, Collier Macmillan, London, 1967.